OXFORD

Sequence analysis

CROSSalive: a web server for predicting the *in vivo* structure of RNA molecules

Riccardo Delli Ponti[1,2], Alexandros Armaos[1,2], Andrea Vandelli[1,2] and Gian Gaetano Tartaglia[1,2,3,4,]*

[1]Gene Function and Evolution, Centre for Genomic Regulation (CRG), The Barcelona Institute of Science and Technology (BIST), Barcelona 08003, Spain, [2]Universitat Pompeu Fabra (UPF), Barcelona 08003, Spain, [3]Institucio Catalana de Recerca i Estudis Avançats (ICREA), Barcelona 08010, Spain and [4]Department of Biology 'Charles Darwin', Sapienza University of Rome, Rome 00185, Italy

*To whom correspondence should be addressed.

Associate Editor: Alfonso Valencia

Abstract

Motivation: RNA structure is difficult to predict *in vivo* due to interactions with enzymes and other molecules. Here we introduce *CROSSalive*, an algorithm to predict the single- and double-stranded regions of RNAs *in vivo* using predictions of protein interactions.

Results: Trained on icSHAPE data in presence (m6a+) and absence of N6 methyladenosine modification (m6a-), *CROSSalive* achieves cross-validation accuracies between 0.70 and 0.88 in identifying high-confidence single- and double-stranded regions. The algorithm was applied to the long non-coding RNA *Xist* (17 900 nt, not present in the training) and shows an Area under the ROC curve of 0.83 in predicting structured regions.

Availability and implementation: *CROSSalive* webserver is freely accessible at http://service.tartaglialab.com/new_submission/crossalive

Contact: gian.tartaglia@crg.es

Supplementary information: Supplementary data are available at *Bioinformatics* online.

1 Introduction

The *in vitro* structure of an RNA differs from that *in vivo* for the action of molecules such as RNA-binding proteins (Livi *et al.*, 2015). The complex mechanisms contributing to the formation of structure *in vivo* are poorly characterized and previous analysis suggests a prevalence of single-stranded regions for all RNA types (Rouskin *et al.*, 2014), although conservation of double-stranded regions has been observed for specific non-coding RNAs (Spitale *et al.*, 2015). In the cellular environment RNA undergoes a number of modifications such as methylation that influence both stability and turnover of the whole transcriptome (Liu and Jia, 2014). *Mettl3* is a key component of the complex that methylates adenosine residues at the N_6 (m6a) and plays a central role in determining RNA structure *in vivo*. Indeed, a method of probing RNA structure using the chemical probe NAI-N3 (icSHAPE) indicated that m6a promotes transition from double- to single-stranded regions (Spitale *et al.*, 2015). Through analysis of icSHAPE data we developed the *CROSSalive* method for the prediction of RNA secondary structure *in vivo*. One important part of our approach is the use of *cat*RAPID predictions of protein interactions to classify single- and double-stranded regions of RNA molecules (Bellucci *et al.*, 2011). *cat*RAPID estimates the binding through van der Waals, hydrogen bonding and secondary structure properties of both protein and RNA sequences.

2 Workflow and implementation

CROSSalive profiles a RNA sequence computing the corresponding secondary structure *in vivo* with (m6a+) and without (m6a-) methylation, which is significantly different from that *in vitro* (Supplementary Fig. S1). The algorithm uses predictions of protein interactions to identify single- and double-stranded regions (Spitale *et al.*, 2015):

- For the training and testing we selected RNA fragments carrying the central nucleotide with the highest (single-stranded; 10^5 non-redundant sequences) and lowest icSHAPE reactivities (double-stranded; 10^5 non-redundant sequences), following the analysis carried out for CROSS *in vitro* (Delli Ponti *et al.*, 2017). Each RNA fragment contains a total of 51 nucleotides to allow calculations with *cat*RAPID (Bellucci *et al.*, 2011). The nucleotides are represented as A = (1, 0, 0, 0), C = (0, 1, 0, 0), G = (0, 0, 1, 0) and U = (0, 0, 0, 1).

- The *cat*RAPID approach uses a phenomenological potential that exploits several physico-chemical predictors including *RNAfold* for the RNA structure (Bellucci *et al.*, 2011). 7797 regions from a library of 640 canonical RNA-binding proteins (Agostini *et al.*, 2013) were analyzed to identify those able to discriminate nucleotides in single- and double-stranded states with accuracies >0.6 (m6a+: 228 regions; m6a-: 206 regions; Supplementary Figs S2 and S3).
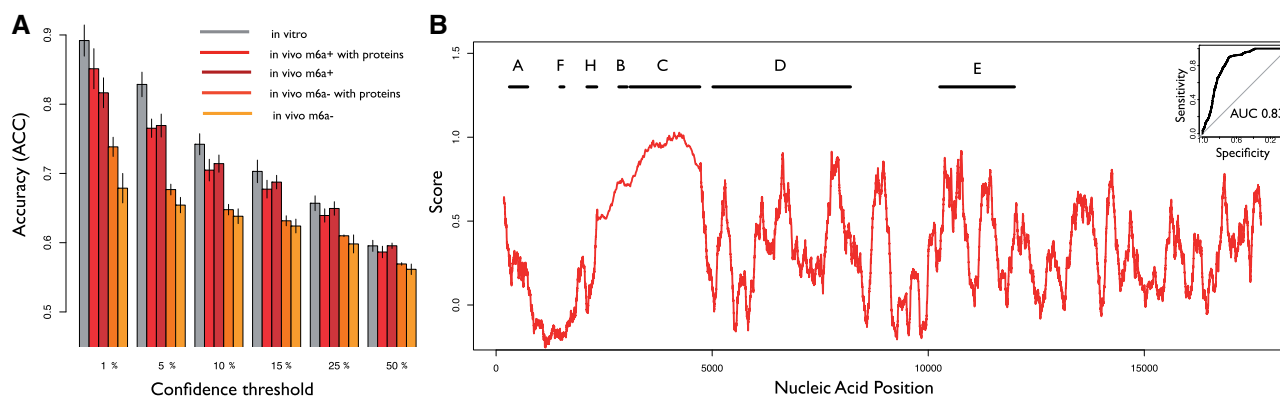
Fig. 1. CROSSalive performances. (**A**) 10-fold cross validation for each specific algorithm (*in vitro*, *in vivo* m6a+, *in vivo* m6a-) with the same training and testing conditions (balanced training set, filtering out sequence redundancy). The accuracies are reported for the scores ranked by their absolute value (same number of positives and negatives were selected), where 50% is the complete set (median). Integrating predictions with protein interactions improves the accuracy. (**B**) Secondary structure profile of *Xist* using m6a- model. Known repetitive regions of *Xist* such as Rep A and Rep C are reported to be very structured (i.e. score > 0). The predicted profile has an overall correlation of 0.45 with *in vivo* SHAPE data. In the top right we report the ROC curve of CROSSalive on the top and bottom 15% ranked SHAPE data (AUC of 0.83)

- The dataset is enriched for proteins with gene ontology (Klus *et al.*, 2015) related to RNA structure (double- and single-stranded RNA binding; helicase activity; m6a+: 101 regions; m6a-: 81 regions; Supplementary Tables S1 and S2). The Youden cut-off was computed on *cat*RAPID scores for each protein in the dataset. Scores above the cut-off were set to 1 (0 otherwise).
- Neural networks (m6a+ and m6a-, with and without protein contributions) were trained using the architecture described in our previous publication for icSHAPE *in vitro* (Delli Ponti *et al.*, 2017). Each RNA fragment is assigned a score between -1 (high propensity to be single-stranded) to 1 (high propensity to be double-stranded; Supplementary Fig. S4).

3 Performances

CROSSalive scores were ranked by their absolute value and equal groups of positives and negatives were selected to assess the performances of the algorithm. From low (50%) to high-confidence (HC) scores (1%, Fig. 1A) the accuracy of the models increases monotonically reaching a maximum of 0.86 for the m6a+ model when protein interactions are used (10-fold cross-validation, CV). In comparison, the *in vitro* icSHAPE model based on RNA sequence information only (Delli Ponti *et al.*, 2017) discriminates single- and double-stranded regions with a 0.88 accuracy (10-fold CV on 1% HC scores). The m6a- *in vivo* model shows lower accuracy (0.74 in 10-fold CV on 1% HC scores) mainly because m6a removal affects the quality of the training set by altering the stability and turnover of the transcriptome (Liu and Jia, 2014). We applied *CROSSalive* to an independent *in vivo* SHAPE-Map experiment (Smola *et al.*, 2016) on the long non-coding *Xist* (17 900 nt; not in the training). We used the *in vivo* m6a- model because *Mettl3* is poorly abundant in the trophoblasts (Thul *et al.*, 2017) employed in SHAPE-Map and only few nucleotides are methylated at the 5′ and 3′ of *Xist* (Patil *et al.*, 2016). The algorithm achieves an Area under the ROC curve (AUC) of 0.83 on the 15% HC single- and double-stranded regions ranked by SHAPE reactivity (Fig. 1B). Moreover, *CROSSalive* profile shows a correlation of 0.45 with the SHAPE-Map one (Fig. 1B). The m6a- model trained on RNA sequence information only achieves an AUC of 0.53 (~0 correlation).

4 Conclusions

By using sequence-based information, *CROSSalive* profiles the RNA secondary structure *in vivo*. The use of different models (*in vivo/in vitro*, m6a+/m6a-) will help to identify structural regions to investigate experimentally. As previously done with *CROSS* (Delli Ponti *et al.*, 2017), *CROSSalive* can be integrated as a constrain in thermodynamics-based approaches such as *RNAfold*, which will allow study structural differences of RNAs *in vivo* and *in vitro* (Lorenz *et al.*, 2016).

References

Agostini,F. *et al.* (2013) catRAPID omics: a web server for large-scale prediction of protein–RNA interactions. *Bioinformatics*, **29**, 2928–2930.

Bellucci,M. *et al.* (2011) Predicting protein associations with long noncoding RNAs. *Nat. Methods*, **8**, 444–445.

Delli Ponti,R. *et al.* (2017) A high-throughput approach to profile RNA structure. *Nucleic Acids Res.*, **45**, e35.

Klus,P. *et al.* (2015) Protein aggregation, structural disorder and RNA-binding ability: a new approach for physico-chemical and gene ontology classification of multiple datasets. *BMC Genomics*, **16**, 1071.

Liu,J. and Jia,G. (2014) Methylation modifications in eukaryotic messenger RNA. *J. Genet. Genomics*, **41**, 21–33.

Livi,C.M. *et al.* (2015) catRAPID signature: identification of ribonucleoproteins and RNA-binding regions. *Bioinformatics*, 773–775.

Lorenz,R. *et al.* (2016) SHAPE directed RNA folding. *Bioinformatics*, **32**, 145–147.

Patil,D.P. *et al.* (2016) m6A RNA methylation promotes XIST-mediated transcriptional repression. *Nature*, **537**, 369–373.

Rouskin,S. *et al.* (2014) Genome-wide probing of RNA structure reveals active unfolding of mRNA structures in vivo. *Nature*, **505**, 701–705.

Smola,M.J. *et al.* (2016) SHAPE reveals transcript-wide interactions, complex structural domains, and protein interactions across the Xist lncRNA in living cells. *Proc. Natl. Acad. Sci. USA*, **113**, 10322–10327.

Spitale,R.C. *et al.* (2015) Structural imprints in vivo decode RNA regulatory mechanisms. *Nature*, **519**, 486–490.

Thul,P.J. *et al.* (2017) A subcellular map of the human proteome. *Science*, **356**, 6340–6352.